The phonon density of states in amorphous materials

2003 J. Phys.: Condens. Matter 15 S2335

(http://iopscience.iop.org/0953-8984/15/31/309)

INSTITUTE OF PHYSICS PUBLISHING JOURNAL OF PHYSICS: CONDENSED MATTER

J. Phys.: Condens. Matter **15** (2003) S2335–S2341 PII: S0953-8984(03)60606-5

The phonon density of states in amorphous materials

M Grimsditch[1], **A Polian**[2] **and R Vogelgesang**[3]

[1] Materials Science Division, Argonne National Laboratory, Argonne, IL 60439, USA
[2] Physique des Milieux Condensés, CNRS, UMR7602, Université P et M Curie, B77, 4 Place Jussieu, 75252 Paris Cedex 05, France
[3] Max Planck Institut für Festkörperforschung, Heisenbergstraße 1, D-70569 Stuttgart, Germany

Received 6 March 2003
Published 23 July 2003
Online at stacks.iop.org/JPhysCM/15/S2335

Abstract

Here we show that the longitudinal (L) and transverse (T) phonon densities of states can be extracted from linearly and circularly polarized Raman spectra. A test of the method for a-Si yields results consistent with the L and T densities of states inferred by analogy with the crystalline state. For a-SiO_2, for which the density of states is not known, both the L and T densities of states are obtained. The results show that the broad peak at around 70 cm^{-1}, commonly called the boson peak, is almost purely T in nature.

(Some figures in this article are in colour only in the electronic version)

1. Introduction

The density of vibrational states in amorphous materials, although it has been the topic of investigation for many decades [1, 2], is still receiving considerable attention. Much of the progress that has been achieved during the past few years is due to the technological improvements in x-ray and neutron inelastic scattering [3–6] and computational techniques [7, 8]. It is noteworthy that most of these recent articles deal with fused silica. So, even for a-SiO_2, which has been extensively investigated, fundamental issues relating to the nature of its vibrational states, are still being discussed.

Raman spectroscopy is known to provide information on the phonon density of states in amorphous materials [1, 2]. It was realized early on that, because the coupling of the vibrations to light is not constant for all modes, Raman spectroscopy yields a 'weighted' density of states, for which the weighting is not accurately known. A few recent investigations have made progress in evaluating the frequency and polarization dependence of the Raman coupling strength [9–11].

Here we present an analysis of the dependence of the Raman coupling strength on the polarization characteristics of the vibrations. On the basis of this analysis we are able to explain the relative intensities of linear and circularly polarized Raman spectra, and we extract, at each frequency, the relative contributions from vibrations with longitudinal (L) and transverse (T)

character. In combination with the density of states obtained from neutron scattering or from simulations, these allow the T and L density of states to be determined.

2. Results

There are two aspects to evaluating the Raman cross-section in amorphous materials: (i) wavevector conservation and (ii) the polarizability changes induced by a given vibration.

The former issue has received most attention to date. An excellent summary of the results has been given in [11]. For vibrations that can be described as damped plane waves of wavevector $\boldsymbol{q}$ and localized around $\boldsymbol{r}_0$

$$\boldsymbol{u} = \boldsymbol{u}_0 \exp(\mathrm{i}\{\boldsymbol{q}\cdot\boldsymbol{r} - \omega t\}) \exp\{-\alpha|\boldsymbol{r} - \boldsymbol{r}_0|\} \tag{1}$$

it can be shown that the interference condition leads to an intensity coefficient $C(\boldsymbol{q})$ proportional to

$$\alpha^2/(\alpha^2 + |\boldsymbol{q} - \boldsymbol{q}_{exp}|^2) \tag{2}$$

where $\boldsymbol{q}_{exp}$ is the experimental scattering wavevector. For zero damping ($\alpha = 0$) this is just the usual delta function $\delta(\boldsymbol{q} - \boldsymbol{q}_{exp})$. Since for the great majority of modes in any material, $\boldsymbol{q} \gg \boldsymbol{q}_{exp}$, it is a good approximation to write $C(q) \approx \alpha^2/(\alpha^2+q^2)$. For an amorphous material, where most modes are expected to be overdamped, this leads to a coupling coefficient that is only weakly frequency dependent. Other assumptions for the localization or attenuation (e.g. a Gaussian packet) lead to variations on the exact form of equation (2); however, they also yield a coupling constant that is only weakly frequency dependent. In [11] it is precisely the frequency dependence of $C(\omega)$ that is used to infer the nature of the phonon localization.

In order to address the issue of the polarization dependence of the coupling, we also describe the vibrations in the amorphous state by damped plane waves. Because of isotropic symmetry of any amorphous material, the displacements of the atoms will, on average, be either L or T relative to the direction of $\boldsymbol{q}$. In a coordinate system where the direction of $\boldsymbol{q}$ is along [100] the resulting strains ($e_{ix} = \mathrm{d}u_i/\mathrm{d}x$) produced by these vibrations are e_{xx}, e_{yx} and e_{zx}. These strains will in turn produce time-dependent polarizability changes through the elasto-optic constants (p_{ij}). Following the classical theory of Brillouin scattering [12, 13], these polarizability changes lead to scattering tensors (χ):

$$\begin{vmatrix} p_{11} & 0 & 0 \\ 0 & p_{12} & 0 \\ 0 & 0 & p_{12} \end{vmatrix}, \qquad \tfrac{1}{2}(p_{11} - p_{12}) \begin{vmatrix} 0 & 1 & 0 \\ 1 & 0 & 0 \\ 0 & 0 & 0 \end{vmatrix}, \qquad \tfrac{1}{2}(p_{11} - p_{12}) \begin{vmatrix} 0 & 0 & 1 \\ 0 & 0 & 0 \\ 1 & 0 & 0 \end{vmatrix}. \tag{3}$$

The first tensor describes L-like vibrations the second two tensors T-like phonons. For phonons propagating along other directions, the relevant tensor must be obtained by a suitable rotation of the axes.

The intensity of a given mode for incident and scattered polarizations $\boldsymbol{e}_i$ and $\boldsymbol{e}_s$ is given by:

$$I = C|\boldsymbol{e}_i \cdot \mathbf{R}^{-1}\boldsymbol{\chi}\mathbf{R} \cdot \boldsymbol{e}_s|^2 \tag{4}$$

where $\mathbf{R}$ is a rotation matrix and C is the constant discussed in the previous paragraph. In a typical Raman experiment, $\boldsymbol{e}_i$ and $\boldsymbol{e}_s$ are fixed in space, and we require the average of equation (4) over all rotations. The (normalized) averages for the three tensors in equation (3) are summarized in table 1 for four pairs of polarizations (e_i, e_s).

The entries in table 1 represent the relative contributions of L and T modes to the Raman spectrum. For example, shear modes will contribute six times more to the ([1i0], [1$\bar{\mathrm{i}}$0]) polarized spectrum (abbreviated +−) than to the ([1i0], [1i0]) spectrum (++). The results in

Table 1. Directional averages of the intensities described by equation (4) for the three tensors in equation (3) and for four polarization configurations.

e_i	e_s	Abbreviated notation	I_L	$I_{T1} = I_{T2}$
[100]	[100]	VV	$3p_{11}^2 + 4p_{11}p_{12} + 8p_{12}^2$	$(p_{11} - p_{12})^2$
[100]	[010]	VH	$(p_{11} - p_{12})^2$	$3(p_{11} - p_{12})^2/4$
$[1\bar{1}0]/\sqrt{2}$	$[110]/\sqrt{2}$	++	$2p_{11}^2 + 6p_{11}p_{12} + 7p_{12}^2$	$(p_{11} - p_{12})^2/4$
$[1\bar{1}0]/\sqrt{2}$	$[1\bar{1}0]/\sqrt{2}$	+−	$2(p_{11} - p_{12})^2$	$3(p_{11} - p_{12})^2/2$

Table 2. Experimental and calculated intensity ratios for the spectra in figure 1(a).

	I_{+-}/I_{VV} @ 300 cm^{-1}	I_{VH}/I_{VV} @ 300 cm^{-1}	I_{++}/I_{VV} @ 300 cm^{-1}	I_{+-}/I_{VV} @ 480 cm^{-1}	I_{VH}/I_{VV} @ 480 cm^{-1}	I_{++}/I_{VV} @ 480 cm^{-1}
Experiment	0.64	0.31	0.87	1.0	0.45	0.66
Calculation	0.59	0.30	0.71	0.92	0.46	0.54

table 1 also predict that +− spectra should be identical in shape to the VH spectra since they have the same ratio of L to T contributions. The former should also be twice as intense as the latter.

Backscattering Raman spectra from a-Si and a-SiO_2, recorded with linear and circular polarizations, are shown in figure 1. Exact backscattering was used to ensure the best possible polarization selection rules for the incident and scattered light. All spectra entered the spectrometer linearly polarized at 45° to the entrance slits, thus guaranteeing that no instrument function need be included in comparing the intensity of the spectra. At a qualitative level the +− and the VH spectra in figures 1(a) and (b) support the predictions of the previous paragraph: namely, they have the same shape and their intensities are in a ratio of ≈2:1.

On the basis of table 1, we can state that the relative intensities of polarized Raman spectra depend only on a single ratio of the elasto-optic constants; we choose this ratio as p_{12}/p_{11}.

As a test, we first perform a comparison of theory and experiment for a-Si for which the density of states is known by analogy with crystalline Si [1, 2]. As pointed out in [2], the broad peak at 300 cm^{-1} for x-Si, and hence also for a-Si, is due only to L-type modes. Table 1 then predicts that their intensities should be in the ratio given the entries in the column headed I_L. The peak at 480 cm^{-1} on the other hand is made up of one L and two T phonon branches, so the intensities are expected to be $I_L + 2I_T$ from table 1. The experimental intensity ratios, normalized to the VV spectrum, are given in table 2.

Since the elasto-optic constants of a-Si are not known, we least-squares fitted the single parameter p_{12}/p_{11} to produce the best agreement with the six experimentally measured intensity ratios in table 2. The best fit was obtained for $p_{12}/p_{11} = -2.4$ which yields the intensity ratios given in the third row of table 2. The model, with just one fitting parameter, produces good agreement with the experimental values and explains the crossing of the +− and ++ spectra close to 400 cm^{-1} in figure 1(a). It is possible to use the inverse process to extract the fraction of L and T states at each frequency. However, since the value of p_{12}/p_{11} has been fitted to yield agreement at two frequencies and since the density of states of a-Si is already known, this procedure is of limited value.

It is of considerably more interest to use the technique to investigate the archetypal amorphous material a-SiO_2 and determine the nature of its vibrational states. For a-SiO_2 the ratio $p_{12}/p_{11} = (0.27/0.121) = +2.23$ is known [14] and hence the relative intensities of all spectra are predicted by table 1 with no adjustable parameter. For example, for the VV

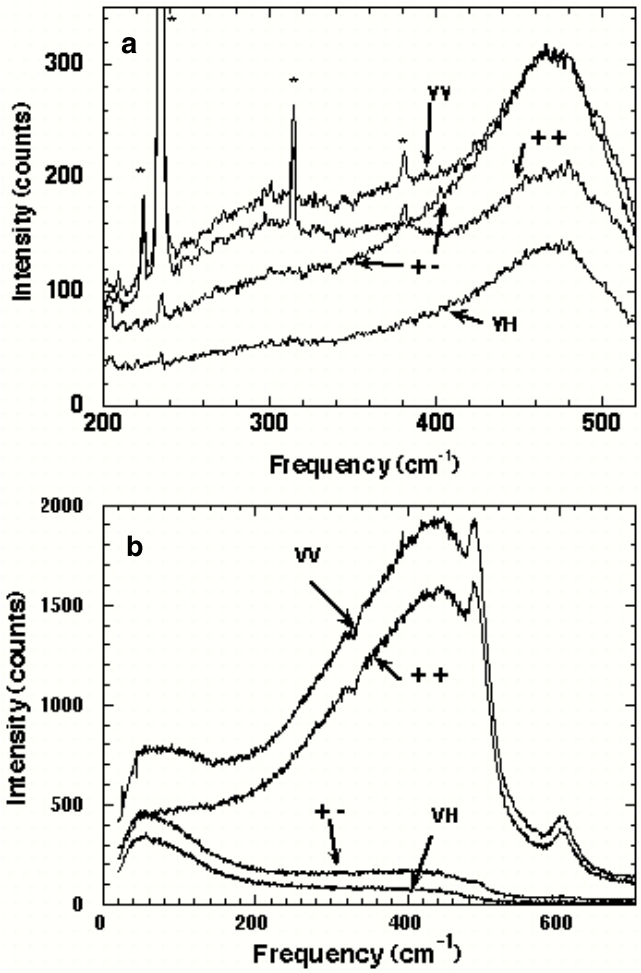

Figure 1. Raman spectra of (a) a-Si and (b) a-SiO_2. The polarizations are abbreviated as follows: VV: linear incident and scattered polarizations parallel to each other; VH: linear incident and scattered polarizations perpendicular to each other; ++: circular incident and scattered polarizations with the same chirality; +−: circular incident and scattered polarizations with opposite chirality. Plasma lines form the laser are indicated by an ∗.

polarization, equation (4) can be rewritten as

$$I_{VV} = C(\omega)[f(\omega)(3p_{11}^2 + 4p_{11}p_{12} + 8p_{12}^2) + (1 - f(\omega))(p_{11} - p_{12})^2] \tag{5}$$

where $f(\omega)$ is the fraction of L modes at frequency ω. Expressions for the other polarizations are straightforward.

Plotted in figure 2(a) is $f(\omega)$ obtained from fitting the four spectra in figure 1(b) to the above equations. Note that the values of f at all frequencies are in the range $0 < f < 1$ as required on physical grounds. Used in conjunction with the density of states, they allow the densities of L and T states to be determined. In figure 2(b) we have plotted (full curve) the calculated density of states (over the same frequency region) from [7]; the product of this density times f (dashed curve) is the density of L modes and the remainder (dotted curve) is the density of T states. It is satisfying to note that the total fraction of L modes in figure 2(b)

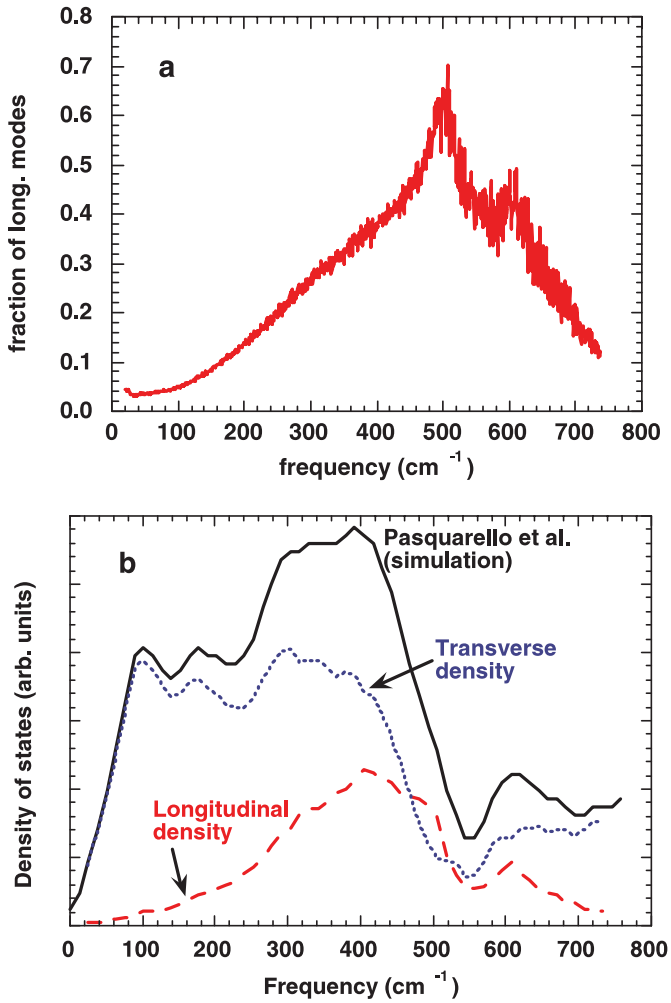

Figure 2. (a) The fraction of long modes. (b) Densities of L and T states.

is 0.26: remarkably close to the expected value 1/3. We stress that there is no parameter in the model that allows the experimental value to be adjusted.

3. Discussion

A comparison of $f(\omega)$ with the spectra in figure 1(b) shows that the low-frequency peak in the spectra is almost purely T in nature. This finding is consistent with the L and T dispersion curves measured for fused silica (figure 15 of [3]). In this vein, the low-frequency peak is a result of nothing more than high density of states associated with the high-frequency end of the T acoustic branch.

The conclusions reached in the preceding section provide some insight as to the origin of the boson peak. This Raman feature is controversial and features prominently [4–6, 11] in many articles dealing with vibrations in amorphous solids. Our understanding is as follows.

The feature at around 70 cm^{-1} in the Raman spectra of a-SiO_2 (figure 1(b)) is the boson peak. Because similar peaks are observed for most glass-forming materials but not for crystals,

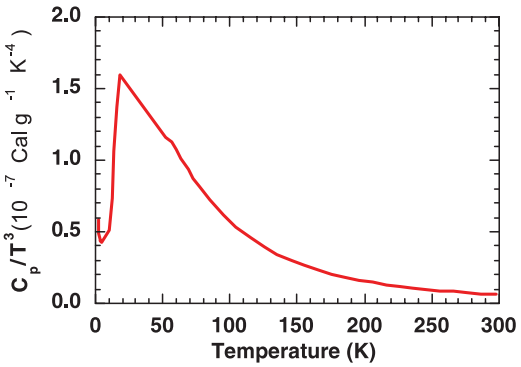

Figure 3. The specific heat of crystalline TiO_2 (rutile) divided by T^3, which exhibits the specific heat anomaly usually associated with glassy materials.

and because it explains the anomalous peak in C_v/T^3 data (a characteristic of many amorphous materials), this feature is often claimed to be an intrinsic feature of glass formation itself. Our views are as follows:

(i) A boson peak is not observed in Raman spectra from crystals simply because of wavevector selection rules. Boson peaks are observed in amorphous materials due to the absence of wavevector selection rules and imply a large density of states at those energies.

(ii) The peak observed in C_v/T^3 in most glasses is termed anomalous since it is inconsistent with the Debye model for the specific heat. What is normally not realized is that most crystals also show an 'anomaly' in C_v/T^3. In figure 3 we have plotted C_v/T^3 for rutile [15]. Diamond also shows an anomaly in C_v/T^3, albeit less pronounced. In both these crystals the anomaly can be traced to the bending over (i.e. deviations from the Debye model) of the T acoustic branch. Hence a specific heat anomaly is not a property of the amorphous state.

(iii) We find that the number of modes associated with the boson peak is roughly $2/3$ of the total number of modes in the system. Since this is what is expected for modes originating in the T acoustic branch of the parent crystal, we see no evidence of 'extra' modes in this region.

In the context of the above arguments, we see no contradiction in the fact that the boson peak simply reflects the high density of states associated with the T acoustic branch. In this picture the boson peak does not reflect any property that is intrinsic to the amorphous or glassy state.

4. Conclusions

We have shown that by suitably combining Raman spectra recorded in different polarization configurations, it is possible to extract the phonon density of states. It is also possible to determine the L or T nature of the features that appear in the density of states. For a-Si the procedure leads to results consistent with its known density of states. For a-SiO_2 it yields a quantitative estimate of the density of states. In particular, it identifies the Raman feature at $\approx$70 cm^{-1}, commonly called the boson peak, as predominantly due to T vibrations.

Acknowledgments

The submitted manuscript was created by the University of Chicago as Operator of Argonne National Laboratory ('Argonne') under Contract No W-31-109-ENG-38 with the US Department of Energy.

References

[1] See for example chapter VI of
Zallen R 1983 *The Physics of Amorphous Solids* (New York: Wiley)
[2] Brodsky M H and Cardona M 1978 *J. Non-Cryst. Solids* **31** 81
[3] Ruocco G and Sette F 2001 *J. Phys.: Condens. Matter* **13** 9141
[4] Foret M, Vacher R, Courtens E and Monaco G 2002 *Phys. Rev.* B **66** 024204
[5] Pilla O *et al Phil. Mag.* B **82** 223
[6] Nakamura M, Arai M, Inamura Y, Otomo T and Bennington S 2002 *Phys. Rev.* B **66** 024203
[7] Pasquarello A, Sarnthein J and Car R 1998 *Phys. Rev.* B **57** 14133
[8] Umari P and Pasquarello A 2002 *Physica* B **316/317** 572
[9] Benassi P *et al* 1995 *Phys. Rev.* B **52** 976
[10] Novikov V *et al* 2002 *Europhys. Lett.* **57** 838
[11] Surovtsev N and Sokolov A P 2002 *Phys. Rev.* B **66** 054205
[12] Born M and Huang K 1968 *Dynamical Theory of Crystal Lattices* (London: Oxford University Press)
[13] Cummins H Z and Schoen P 1972 *Laser Handbook* ed F Arecchi and E O Schulz-Dubois (Amsterdam: North-Holland) p 1029
[14] Dixon R W 1967 *J. Appl. Phys.* **38** 5149
[15] Touloukian Y S T and Buyco E H (ed) 1970 *Thermophysical Properties of Matter (Specific Heat vol 5)* (New York: Plenum)